The Output State of a Quantum Computer

Daniel Bloch
Department of Electrical Engineering and Computer Science
Florida Atlantic University
Boca Raton, United States
dbloch2017@fau.edu

Faculty Mentors

Dr. Maria Petrie
Department of Electrical Engineering and Computer Science
Florida Atlantic University
Boca Raton, United States
petrie@fau.edu

Dr. Korey Sorge
Department of Physics
Florida Atlantic University
Boca Raton, United States
ksorge@fau.edu

***Abstract*—This study explores a comprehensive overview of quantum computing hardware, emphasizing qubit creation and measurement, which are essential for advancing quantum computing and its applications. Quantum computing stands at the forefront of technological advancement, offering unprecedented computational power and the potential to address complex problems beyond classical computing systems' capabilities. Inspired by Schrödinger's Cat thought experiment, this study employs an experimental apparatus enabling observers to generate quantum mechanical wavefunctions, acquire precise measurements, and analyze resulting binary output states, consisting of either a '0' or a '1'. The primary objective is to investigate the generation of binary combinations and determine the probability distribution of the resulting output states. The results are then compared with IBM's quantum computer data to validate these findings. Ultimately, this research advances comprehension of quantum computing and its potential impact on the technological landscape. It aims to expand knowledge and pave the way for advancements and innovation in quantum computing, benefiting various applications across diverse domains.**

***Index Terms*—quantum computing, wavefunction, superposition**

I. Introduction

Quantum physics is beautiful and weird. Understanding the nature of reality at the most miniature scale expands our understanding of the universe, where the observer plays a central role in shaping reality.

In his 1982 paper "Simulating Physics with Computers," Richard Feynman posed a fundamental question: "Can physics be simulated by a universal computer?" [1] This inquiry delves specifically into the simulation of quantum physics, wherein algorithms are designed to solve differential equations, effectively predicting the behavior of physical systems [1]. Feynman explores the concept of simulating space and time, abstracting away from the hardware specifics of computers. For this to work, the computer must understand nature and work as nature does, thus suggesting the idea of quantum computing [1].

This study draws upon the foundational principles introduced by Erwin Schrödinger's Cat thought experiment, leveraging modern technology to substantiate its findings [2]. An observer initiates a quantum wavefunction, indicating that the system exists in superposition while the specific state remains undetermined. A qubit—the fundamental unit of information—can simultaneously exist in multiple states [3]. Upon measurement, the wavefunction collapses, yielding a binary output state of either '0' or '1'.

II. Background Theory

A. The Potential

Today, major companies like IBM and Google are racing to advance quantum computing technologies, heralding a potential revolution in computational capabilities [4]. The current functionality of these systems enables users to craft simulations, like quantum circuits, and transmit them over the internet for processing by quantum computers. With quantum computing research and development growth fueled by significant investments and collaborations across academia and industry, the prospects for achieving this transformative vision have never been more promising. These companies envision a future where quantum computers unlock solutions to classically intractable problems, promising a paradigm shift in computation.

However, beyond the excitement of running simulations on cutting-edge hardware, questions linger: What sets quantum computing apart? What lies beyond merely simulating code on powerful machines?

B. The Architecture

The superconducting quantum computing system model illustrated in Figure 1, as provided by Qfinity Labs [5], not only serves as a technical blueprint but also unveils profound

This research was funded by the Florida Atlantic University Office of Undergraduate Research and Inquiry

implications for computing. While researchers and engineers invest resources in simulating its probabilistic behavior, complexities persist. As Albert Einstein famously remarked, "God doesn't play dice with the universe," highlighting the challenges of governing physical laws with complex machinery and the uncertainties it introduces to our investments [6]. In response, Niels Bohr's said to Einstein, "Stop telling God what to do," offers insight into how, despite encountering setbacks and uncertainties in our pursuit, this exploration deepens our comprehension of the universe's fundamental fabric and our role within it [6].

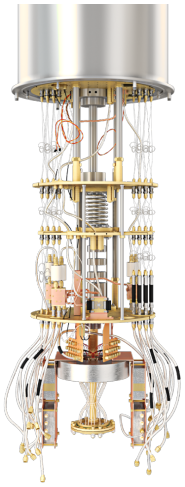

Fig. 1. Model of a superconducting quantum computer. [5]

The shell is found in Figure 2, which is a vacuum-sealed container that maintains near sub-zero temperatures throughout the computer [5]. This measure helps prevent decoherence, where environmental factors influence the system's behavior. When a qubit is decoherent, this introduces an unwanted element of uncertainty into a quantum computer [7]. There is no way to predict the result of another measurement [7]. The process of maintaining an ideal state is similar to Bose-Einstein condensates [8]. Currently, in the International Space Station, these particles are in anti-gravity, near sub-zeroed cooled chambers that allow the system to exist in its preferred environment [9]. Having the ideal conditions can best evaluate a system that generates quantum weirdness.

Fig. 2. The shell. [5]

The near sub-zero temperatures required for cooling the quantum computer components are achieved through specialized refrigeration systems, such as cryogenic cooling systems. Additionally, the vacuum-sealed shell isolates the interior from external heat sources, thereby assisting in maintaining the desired low temperatures [5].

The nerves found in Figure 3, sometimes termed "microwave lines" serve as the connective tissue within a quantum computer [10]. They facilitate the transmission of signals to and from the qubits, enabling the execution of quantum operations, and subsequently conveying the outcomes [7].

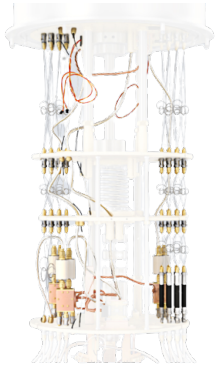

Fig. 3. The nerves. [5]

The heart, as seen in Figure 4, is a mixing chamber that houses different forms of liquid helium, including ^{3}He (helium-3) and ^{4}He (helium-4), because these substances possess unique thermodynamic properties that make them ideal for cooling purposes [5]. ^{3}He and ^{4}He are both isotopes of helium with different properties. ^{4}He, a boson, follows Bose-Einstein statistics [11]. When the temperature of pure ^{4}He is below 2.17 K at saturation vapor pressure, the ^{4}He transforms from helium-I to helium-II [11]. This process is commonly used for its thermal conductivity and ability to remain in a liquid state at very low temperatures ($T < 0.7$ K) [11].

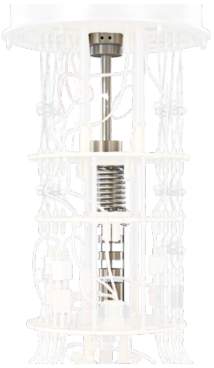

Fig. 4. The heart. [5]

"The ^{3}He in a ^{3}He-^{4}He mixture is regarded as a weakly-interacting Fermi gas" [11]. When the temperature is lower

than 0.87 K, phase separation leads to a concentrated and dilute phase [11]. The concentration is almost pure when the temperature is near 0 K, allowing dilution to occur at very low temperatures [12]. The ^{3}He leaves the mixing chamber, flows through the heat exchangers in the dilute phase and cools the incoming liquid [11].

The skeleton in Figure 5 contains gold plates that serve as separators between the cooling zones [5]. In the top chamber, the temperature is maintained below absolute zero, approximately -273.15 degrees Celsius [13]. This extremely low temperature is necessary to facilitate the quantum processes occurring within the system. Descending towards the bottom of the chamber, the temperature drops even further, reaching one-hundredth of a kelvin [13].

Fig. 5. The skeleton. [5]

The Quantum Processing Unit (QPU) in Figure 6 is an essential component within the quantum computer architecture. Its physical structure consists of a gold-plated copper disk, carefully engineered to provide stability and conductivity essential for quantum operations [5]. Encased within this disk is a silicon chip designed to house the quantum computer's computational core or "brain" [14]. The silicon chip contains an array of qubits and control mechanisms, allowing for the execution of quantum algorithms and computations [15]. This configuration enables the QPU to use the behavior of particles to make certain kinds of calculations much faster than processors in today's computers. "The practical implementation of quantum processing is anticipated to necessitate tens of thousands of qubits or even more to address real-world problems effectively" [16]. However, determining the precise problem sizes at which quantum systems will outperform conventional computing systems remains largely uncertain, primarily due to the impact of engineering limitations on QPU performance [16]. Moreover, it's essential to underscore the transformative potential that Quantum Processing Units possess. "Quantum processing units have the potential to revolutionize various fields such as cryptography, quantum simulations, machine learning and solve complex optimization problems" [15]. While QPUs are still in their early era of making a substantial impact in addressing real-world problems, with diligence and time, they have the potential to act as engineering marvels and solve the problems we are looking to solve.

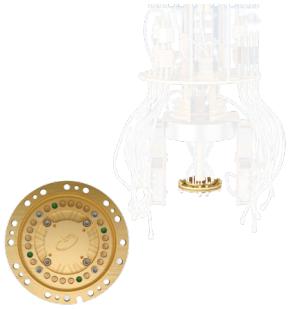

Fig. 6. The brain. [5]

III. Experimental Approach

The experiment aimed to measure the resulting output state of a quantum computer.

A. Apparatus

When the Quantum Wavefunction Generator in Figure 7 is powered, the two laser sources are visible, indicating a generated wavefunction. Integrated within the system is a button that triggers the collapse of the wavefunction, revealing the system's current state to the observer. The laser will shut off indicating the collapse, then turn back on to regenerate the wavefunction. While the generated wavefunction is apparent, the observer is unaware of the system's current state; upon deactivation, indicating a collapsed wavefunction, the binary state of either '0' or '1' is presented to the observer.

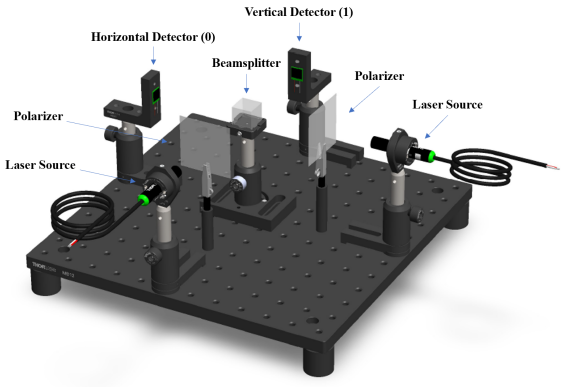

Fig. 7. Quantum Wavefunction Generator

The two laser sources emit light at a wavelength of 520 nm, with each beam directed towards a polarizer to precisely align its polarization. This alignment guarantees that the light waves oscillate uniformly in a specific orientation, ensuring predictability when interacting with optical components and preventing undesirable back reflections [17]. The beamsplitter directs the polarized light. When the light reaches the detectors, it splits, with half reflecting towards the horizontal detector and the remaining half transmitting towards the vertical detector [18].

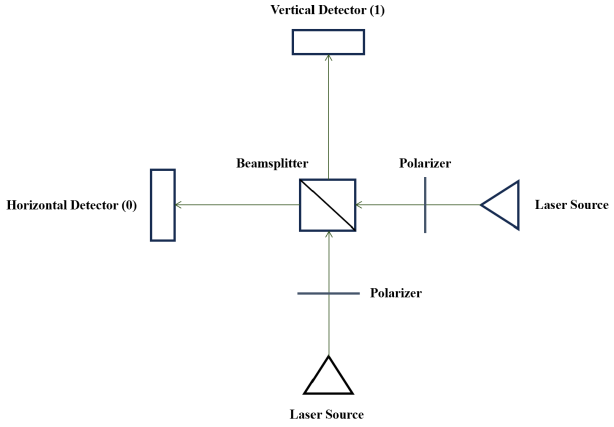

Fig. 8. Quantum Wavefunction Generator diagram

However, a photon embodies a single quantized energy state, represented by Equation 1 [18].

$$E = hf \tag{1}$$

E is the energy, h is Planck's constant ($6.55 \times 10^{-34} J \cdot s$), and f is the photon's frequency. The photon cannot be divided and will only follow a discrete path [18]. Consequently, it is equally likely to be detected at either the horizontal detector, leaving an output state of '0', or at the vertical detector, leaving an output state of '1'.

This observation might suggest that each photon follows a distinct path—vertically or horizontally—randomly chosen [18]. However, by quantum mechanics principles, a photon traverses both paths simultaneously, only collapsing into a single path upon measurement ("the collapse of the wavefunction") [18]. The experimental setup evaluates a continuous stream of photons and develops an electric power generation system. This system analyzes each state's gradual energy increase over time.

B. Equations

By employing a 520 nm photoresistor for the detectors (*LDR1*), interconnected in series with a resistor (*R*1), followed by a load resistor (R_L) connected to ground, this establishes a voltage divider circuit, as seen in Figure 9. The photoresistor's resistance changes with light intensity, causing the voltage at the junction between the two resistors to vary. The voltage drop across the photoresistor ($V_{photoresistor}$), denoted by Equation 2, is determined by scaling the digital reading ($V_{digital}$) obtained from the analog pin to a voltage value and subtracting it from the total voltage at the junction between the two resistors. This process provides the voltage specifically across the photoresistor from the light intensity. To mirror the circuit for the second detector, the setup of Figure 9 is replicated by employing another 520 nm photoresistor (*LDR2*), interconnected in series with a resistor (*R2*), followed by a load resistor (R_L) connected to ground.

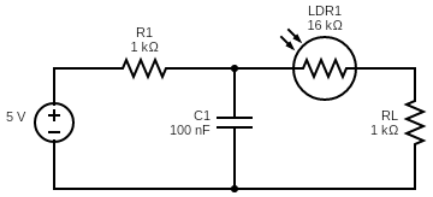

Fig. 9. Quantum Wavefunction Generator circuit for detectors

$$V_{photoresistor} = V_{junction} - \frac{V_{digital} \times V_{junction}}{1024} \tag{2}$$

The power consumed by the photoresistor ($P_{photoresistor}$) is then determined by squaring the voltage across the photoresistor, divided by the resistor load.

$$P_{photoresistor} = \frac{V^2_{photoresistor}}{R_L} \tag{3}$$

By tracking power consumption within 500 ms intervals, energy assessment (ΔE) involves multiplying the power of the photoresistor (p) by the time difference between t_i and t_{i-1} (ΔT).

$$\Delta E = p\Delta T \tag{4}$$

Ultimately, the final output state is based on the highest energy level detected by the horizontal and vertical detectors when the observer collapses the wavefunction, symbolizing '0' and '1', respectively.

The probability is calculated by dividing the total number of occurrences in each state by the total shots conducted in the experiment. Regarding quantum computing, a shot represents the number of times the circuit executes.

$$\text{Probability} = \frac{\text{Number of Occurrences in a State}}{\text{Total Number of Shots}} \tag{5}$$

The state vector represents the state of a quantum system and is represented by Equation 6.

$$|\psi\rangle = \alpha|0\rangle + \beta|1\rangle \tag{6}$$

Where,

$$\alpha = cos(\frac{\theta}{2}) \tag{7}$$

and

$$\beta = e^{i\phi} sin(\frac{\theta}{2}) \tag{8}$$

α and β represent the probability amplitudes. They contain both the magnitude (related to the probability of measuring the state) and the phase of the quantum state [19]. $|\alpha|^2$ and $|\beta|^2$ represent the probabilities of measuring the qubit in the states $|0\rangle$ and $|1\rangle$, respectively.

C. Simulation

A quantum circuit was employed to match the experimental apparatus. Figure 10 has a qubit applied with a Hadamard gate. The Hadamard gate is a quantum logic gate that creates a superposition of states. Upon measurement, the wavefunction collapses, allowing the observer to ascertain the system's binary state.

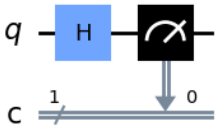

Fig. 10. Quantum circuit diagram illustrating the application of a Hadamard gate to a qubit, inducing a superposition state, followed by measurement. [Source: Qiskit]

IV. Results

Below are the output states obtained from the experimental apparatus and a simulated quasi-probability distribution generated by IBM's quantum computer.

The findings presented in Figure 11 illustrate the dynamic fluctuations in the system's states over time following the collapse of the wavefunction. These fluctuations reveal various energy levels, with the highest indicating the resulting output state. Notably, the states exhibit similar energy levels, suggesting an optimal system characterized by a superposition of states.

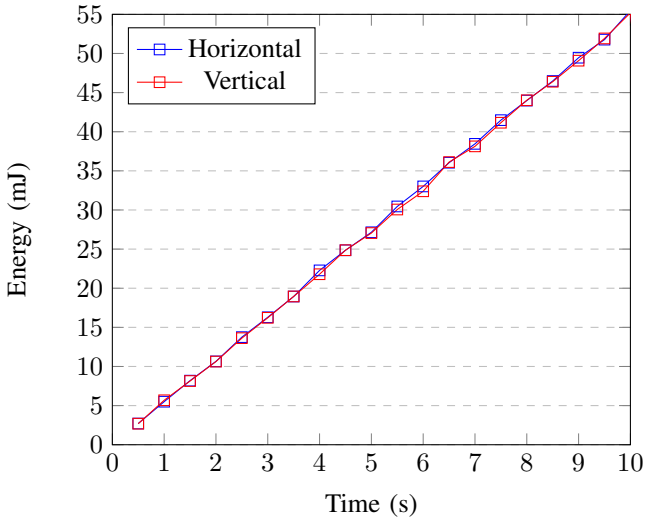

Fig. 11. Energy change of the Quantum Wavefunction Generator over 10 s for each detector

It is important to note that the system accumulates energy over time. Schrödinger's thought experiment contains a radioactive element. Once the Geiger counter detects radiation, the hammer drops and releases poison to that cat. Essentially, the system accumulates energy over time, directly impacting the system's state.

Table I provides insights into the observations made by the observer following the collapse of the wavefunction. This observation spans 10 seconds, with measurements taken at 500 ms intervals. It details the instantaneous power consumption of each detector, the cumulative energy acquired by the system over time, the time elapsed, and the resulting output state. A 500 ms delay is implemented to ensure the detectors make precise recordings.

TABLE I
Output States

States	**Power H** (mW)	**Power V** (mW)	**Energy H** (mJ)	**Energy V** (mJ)	**Total Time** (m:s:ms)
0	5.42	5.38	2.71	2.69	0:00:500
1	5.84	6.19	5.50	5.68	0:01:000
0	5.71	5.65	8.19	8.14	0:01:500
0	5.17	5.08	10.65	10.63	0:02:000
0	5.48	5.44	13.75	13.62	0:02:500
0	5.41	5.46	16.29	16.22	0:03:000
1	5.33	5.35	18.94	18.95	0:03:500
0	5.46	5.46	22.28	21.79	0:04:000
1	5.46	5.44	24.85	24.86	0:04:500
0	5.63	5.59	27.15	27.05	0:05:000
0	5.37	5.37	30.45	30.06	0:05:500
0	5.46	5.37	33.01	32.39	0:06:000
1	5.39	5.38	36.04	36.12	0:06:500
0	5.37	5.36	38.45	38.13	0:07:000
0	5.36	5.32	41.48	41.15	0:07:500
1	5.79	5.72	43.98	44.02	0:08:000
0	5.39	5.35	46.48	46.39	0:08:500
0	5.36	5.32	49.46	49.08	0:09:000
1	5.31	5.35	51.77	51.92	0:09:500
0	5.35	5.32	55.49	55.19	0:10:000

The probability of acquiring the '0' state is:

$$14/20 = 0.70 \tag{9}$$

The probability of acquiring the '1' state is:

$$6/20 = 0.30 \tag{10}$$

The simulation of Figure 10 was run on IBM's quantum computer for 20 shots. After the circuit was executed, the number of counts was given for each state. The observer received fourteen 0s and six 1s, thereby validating the superposition state of the Quantum Wavefunction Generator with a quantum computer. The quasi-probability distribution can be seen in Figure 12.

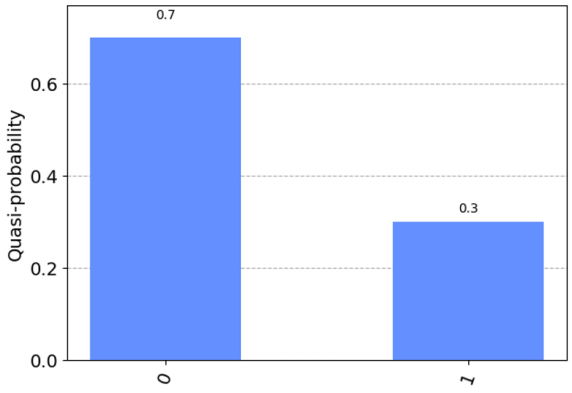

Fig. 12. Quasi-probability distribution over 20 shots. [Source: Qiskit]

Equation 11 is the state vector with the probabilistic value corresponding to the observable being measured. These values are implemented into the equation, thereby representing the system's quantum state.

$$|\psi\rangle = \sqrt{0.70}|0\rangle + \sqrt{0.30}|1\rangle \tag{11}$$

The Bloch sphere, as seen in Figure 13, provides a visual representation of the state of a quantum system. By applying the state vector, the resulting probabilistic outcomes of the superstition state yield a higher probability for the collapsed measurement to be a binary '0' rather than a '1'. From analysis, the system exists in superposition, and its resulting state vector is derived from the output states.

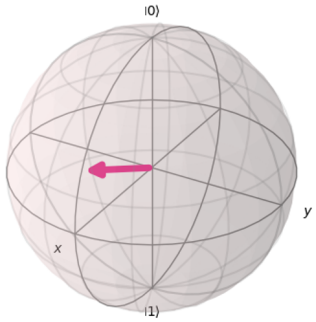

Fig. 13. Bloch sphere representation of the quantum state in superposition. [Source: Qiskit]

Conclusion

While an observer does not perceive a superposition of states when collapsing a wavefunction through measurement, they can observe probabilistic outcomes corresponding to the observable being measured. These outcomes are determined by the superposition coefficients, which dictate the probability of observing each outcome. Once the wavefunction collapses, the probability distribution of the output state of the system changes. Initially, the observer is unaware of the system's output state, as it exists in an equal probabilistic state. However, the system's state is revealed upon collapsing the wavefunction, providing the observer with the data necessary to understand its configuration.

Future Directions

Utilizing the experimental apparatus and knowledge gained from this study, the future direction involves exploring the application of quantum dots in cancer therapy.

Acknowledgment

- Office of Undergraduate Research and Inquiry for funding and supporting this research project.
- Dr. Mahsa Ranji from the Biophotonics Lab, Florida Atlantic University, for providing the space and resources needed for this project.
- Perry C. Weinthal from the Electrical Engineering Lab, Florida Atlantic University, for supplying the necessary hardware and guidance.

References

[1] R. Feynman, "Simulating Physics with Computers," *International Journal of Theoretical Physics*, vol. 21, pp. 467–488, May 1981.

[2] S. Metwalli, "What is Schrödinger's Cat?," *builtin*, https://builtin.com/software-engineering-perspectives/schrodingers-cat#:~:text=Schr%C3%B6dinger's%20Cat%2C%20as%20a%20thought,until%20you%20open%20the%20box (accessed Mar. 23, 2024).

[3] "What is a Qubit?," *University of Waterloo*, https://uwaterloo.ca/institute-for-quantum-computing/quantum-101/quantum-information-science-and-technology/what-qubit (accessed Apr. 4, 2024).

[4] K. Hartnett, "Google and IBM Clash Over Milestone Quantum Computing Experiment," *Quantum Magazine*, https://www.quantamagazine.org/google-and-ibm-clash-over-quantum-supremacy-claim-20191023/ (accessed Mar. 23, 2023).

[5] D. Moche, Qfinitiy Labs, qfinitylabs.com (accessed Mar. 3, 2023).

[6] S. Soko, "The War on Quantum Theory: Albert Einstein and Niels Bohr," *Girls in Quantum*, https://girlsinquantum.com/the-war-on-quantum-theory-albert-einstein-and-niels-bohr/ (accessed Mar. 23, 2024).

[7] N. Quesnel, "Quantum Computing Cooling," *Advanced Thermal Solutions, INC.*, https://www.qats.com/cms/2019/08/02/quantum-computing-cooling/ (accessed Mar. 23, 2024).

[8] M. Schwartz, "Lecture 12: Bose-Einstein Condensation," *Harvard University*, https://scholar.harvard.edu/files/schwartz/files/12-bec.pdf (accessed Apr. 4, 2024)

[9] "Bose-Einstein Condensate is Made Onboard the International Space Station," *Physics World*, https://physicsworld.com/a/bose-einstein-condensate-is-made-onboard-the-international-space-station (accessed Apr. 9, 2024).

[10] J. C. Bardin, D. H. Slichter and D.J. Reilly, "Microwaves in Quantum Computing", *Atomic Energy Research Establishment*, Harwell, England, vol. 128, Dec. 1962.

[11] H. Zu, W. Dai and A.T.A.M. de Waele, "Development of Dilution Refrigerators—A Review," *Elsevier*, May 1981.

[12] H. London, G. R. Clarke, and E. Mendoze, "Osmotic Pressure of He-3 in Liquid He-4, with Proposals for a Refrigerator to Work Below 1-Degrees K", *IEEE Journal of Microwaves*, vol. 1, October 2020.

[13] J. Shepard, "Why Use Attenuators in Quantum Computers?," *Analog IC Tips*, https://www.analogictips.com/why-use-attenuators-in-quantum-computers-faq/#:~:text=Cryo%20attenuators%20are%20used%20on,to%20creep%20into%20the%20system. (accessed Mar 23, 2024).

[14] MOONSHOT Research and Development Program, "Quantum Computing System," *Japan Science and Technology Agency*, https://www.jst.go.jp/moonshot/en/program/goal6/appeal/65_mizuno_ap01.html (accessed Mar. 23, 2024).

[15] R. Merritt, "What is a QPU?," *NVIDIA*, https://blogs.nvidia.com/blog/what-is-a-qpu/ (accessed Mar. 23, 2024).

[16] K. Britt and T. Humble, "Instruction Set Architectures for Quantum Processing Units", *Oak Ridge National Laboratory*, Jul. 2017.

[17] "The Science of Thin Film Polarizers in Laser Systems", *Blue Ridge Optics* https://blueridgeoptics.com/thin-film-polarizers-laser-systems/ (accessed Apr. 7, 2024).
[18] Prashant, "A Study on the Basics of Quantum Computing," *University of Montreal*, vol. 1, Dec. 2005.
[19] A. Dawar, "Quantum Computing Lecture 1", *University of Cambridge*, https://www.cl.cam.ac.uk/teaching/0910/QuantComp/notes.pdf (accessed Apr. 9, 2024).